Supplementary

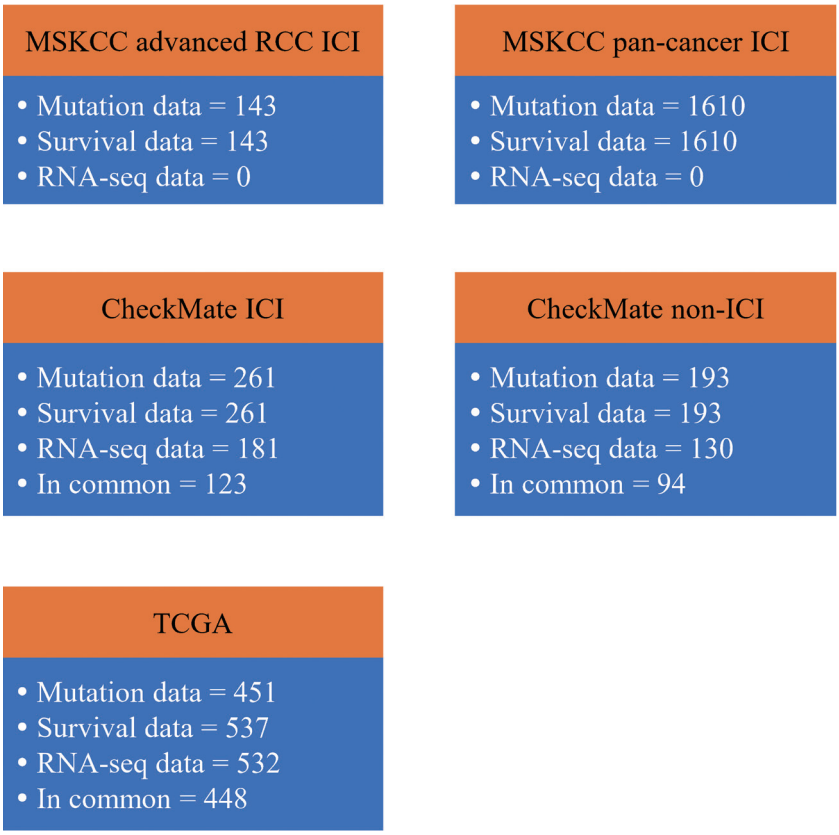

Figure S1 Data sources.

https://dx.doi.org/10.21037/tau-23-21

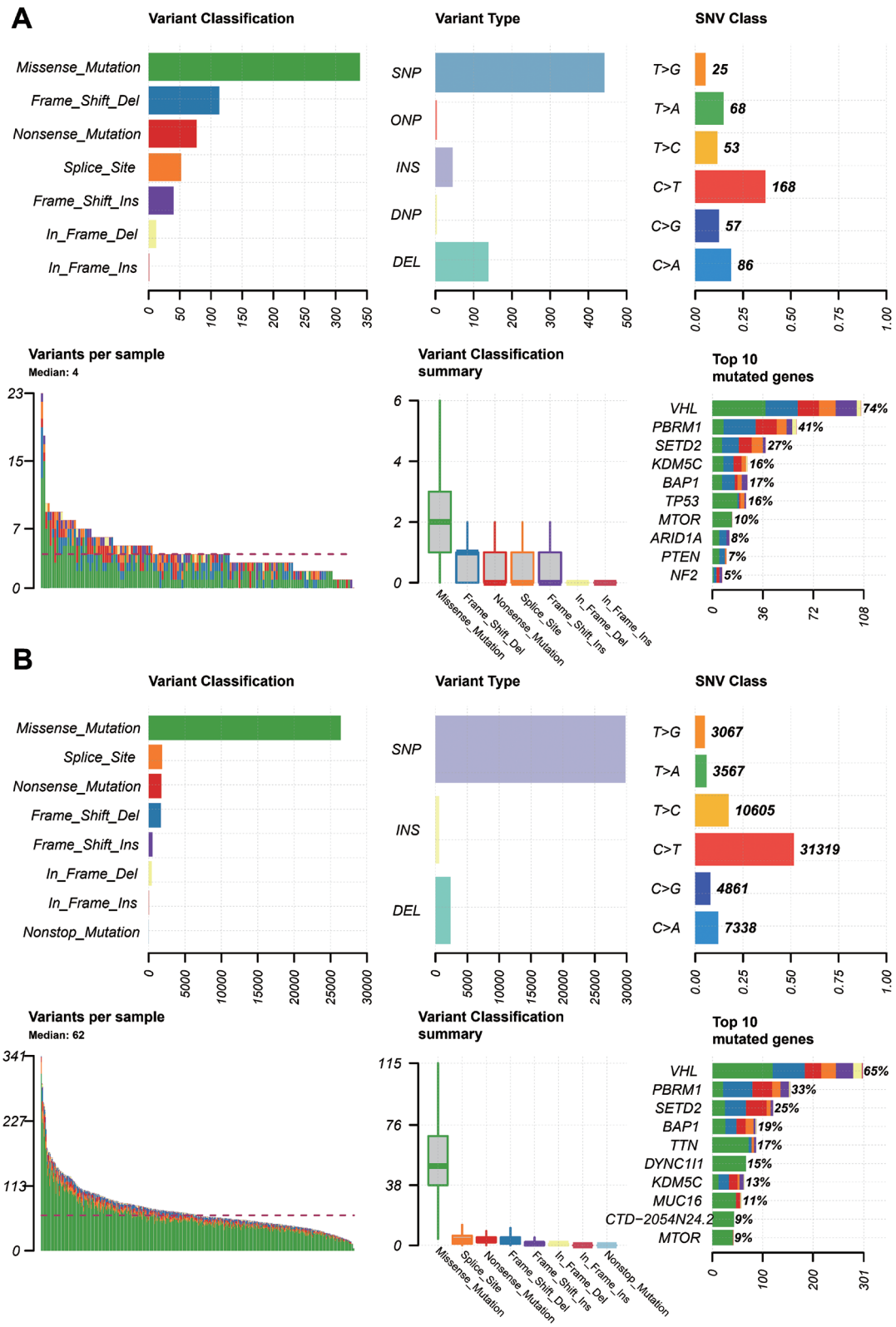

Figure S2 Mutation pattern and frequencies in patients with RCC from the MSKCC advanced RCC ICI therapy cohort (n=143) and the CheckMate ICI therapy cohort (n=261). (A) MSKCC advanced RCC ICI therapy cohort (n=143). (B) CheckMate ICI therapy cohort (n=261).

https://dx.doi.org/10.21037/tau-23-21

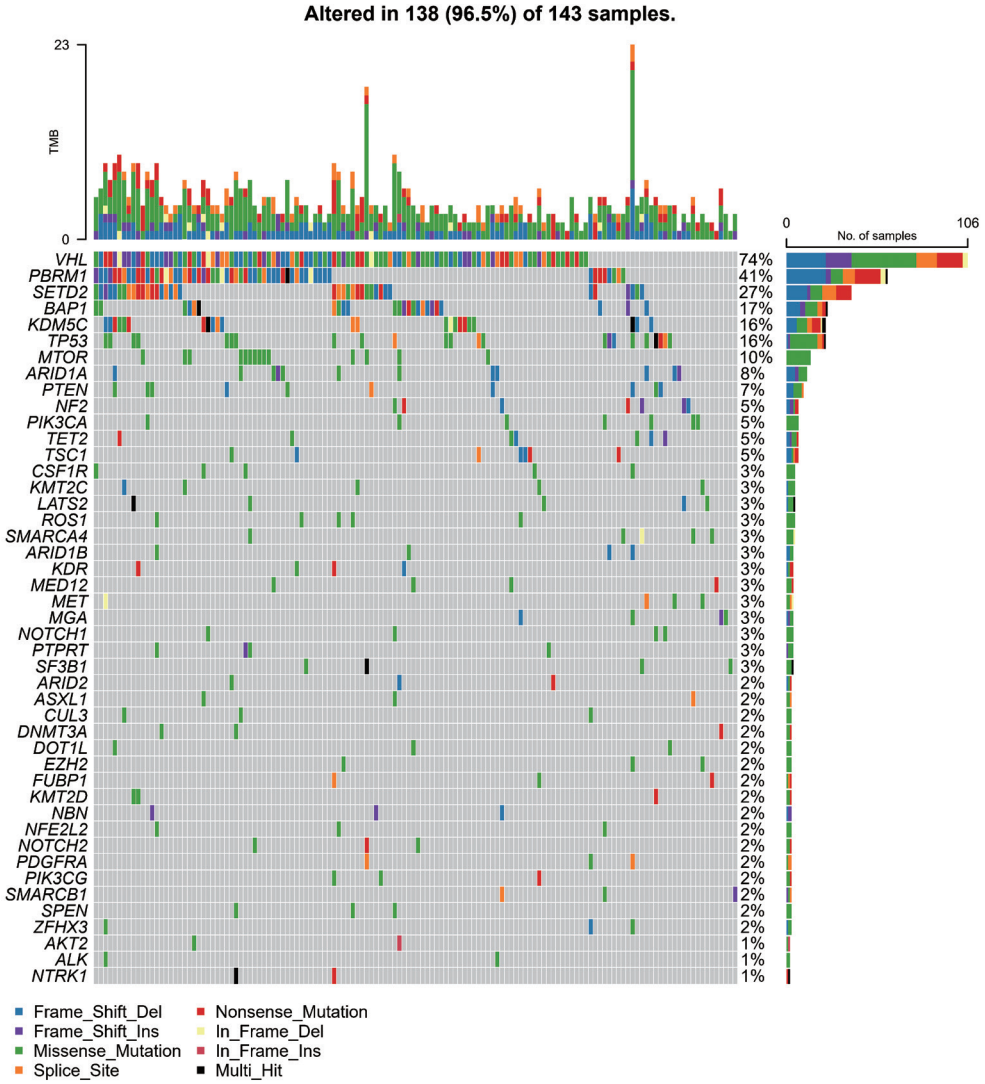

Figure S3 Oncoplot of the top 45 most frequently mutated genes in the MSKCC advanced RCC ICI therapy cohort (n=143).

https://dx.doi.org/10.21037/tau-23-21

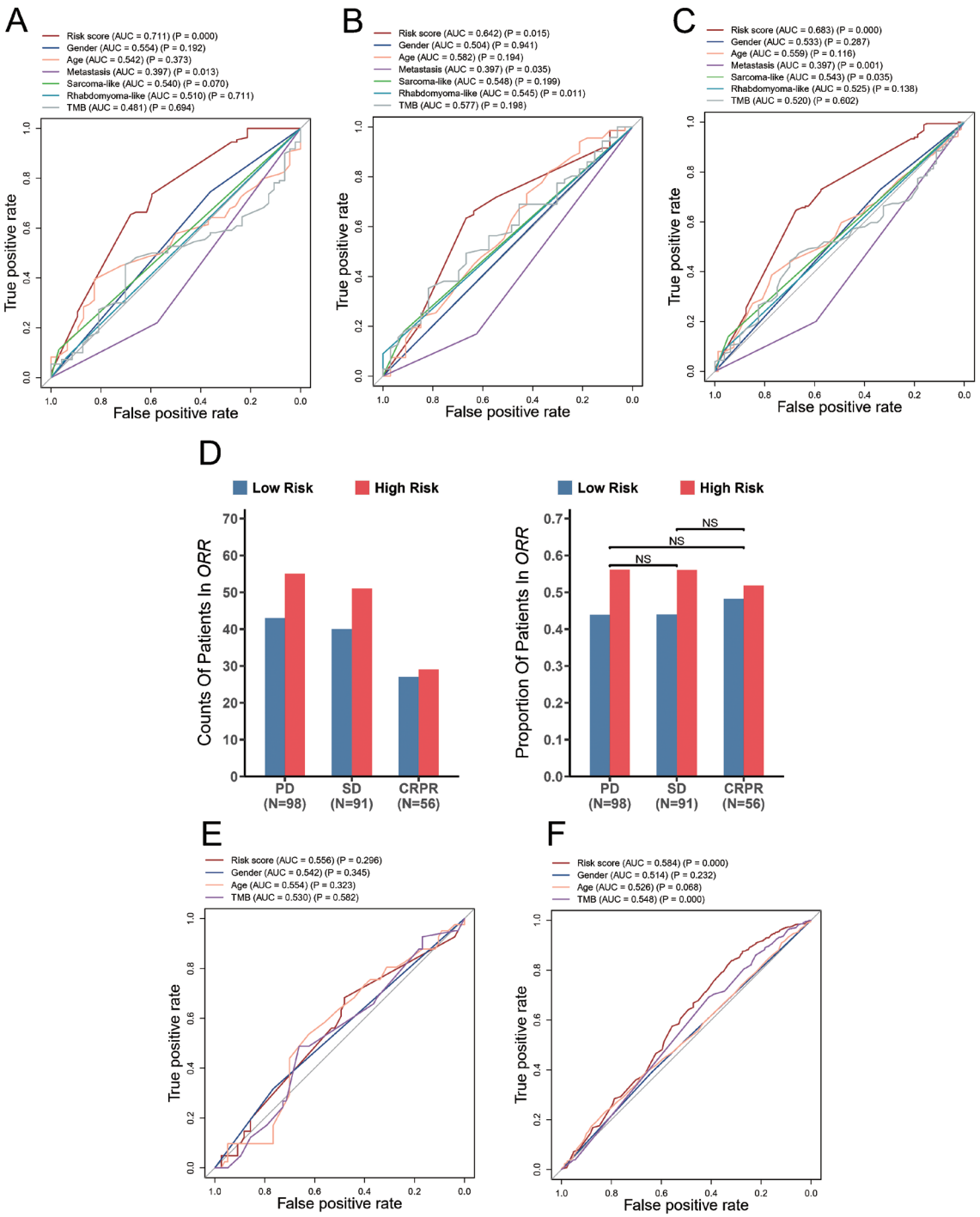

Figure S4 (A-C) Comparison of the risk score with other available clinical factors using ROC analyses based on OS in the CheckMate ICI therapy cohort: (A) training set, (B) validation set, (C) the whole set. (D) Counts and proportion of patients in the CheckMate ICI therapy cohort identified with the 10-gene mutation classifier and stratified by ORR. Patients were stratified by ORR into complete response (CR)/ partial response (PR), stable disease (SD), and progressive disease (PD) subgroups. NS, no significance. (E) ROC curve analysis based on OS in the MSKCC advanced RCC ICI therapy cohort. (F) ROC curve analysis based on OS in the MSKCC pan-cancer ICI therapy cohort.

https://dx.doi.org/10.21037/tau-23-21

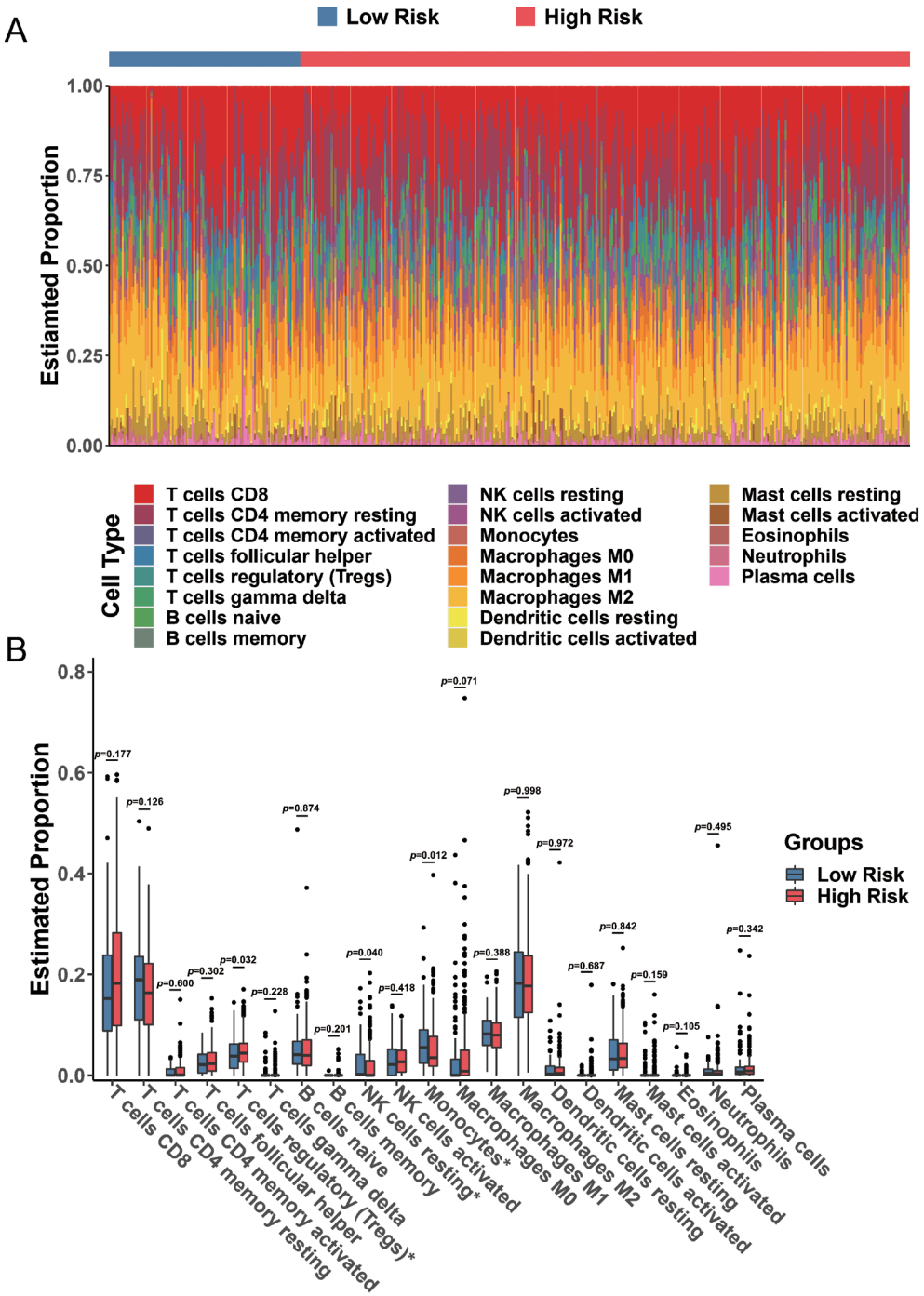

Figure S5 Fraction of 22 tumor-infiltrating immune cells (LM22) in patients in TCGA cohort identified with the 10-gene mutation classifier. (A) The risk groups and proportions of 22 tumor-infiltrating immune cells in the TCGA cohort. (B) Barplot showed the different proportions of 22 tumor-infiltrating immune cells between the low- and high-risk groups in the TCGA cohort.

https://dx.doi.org/10.21037/tau-23-21

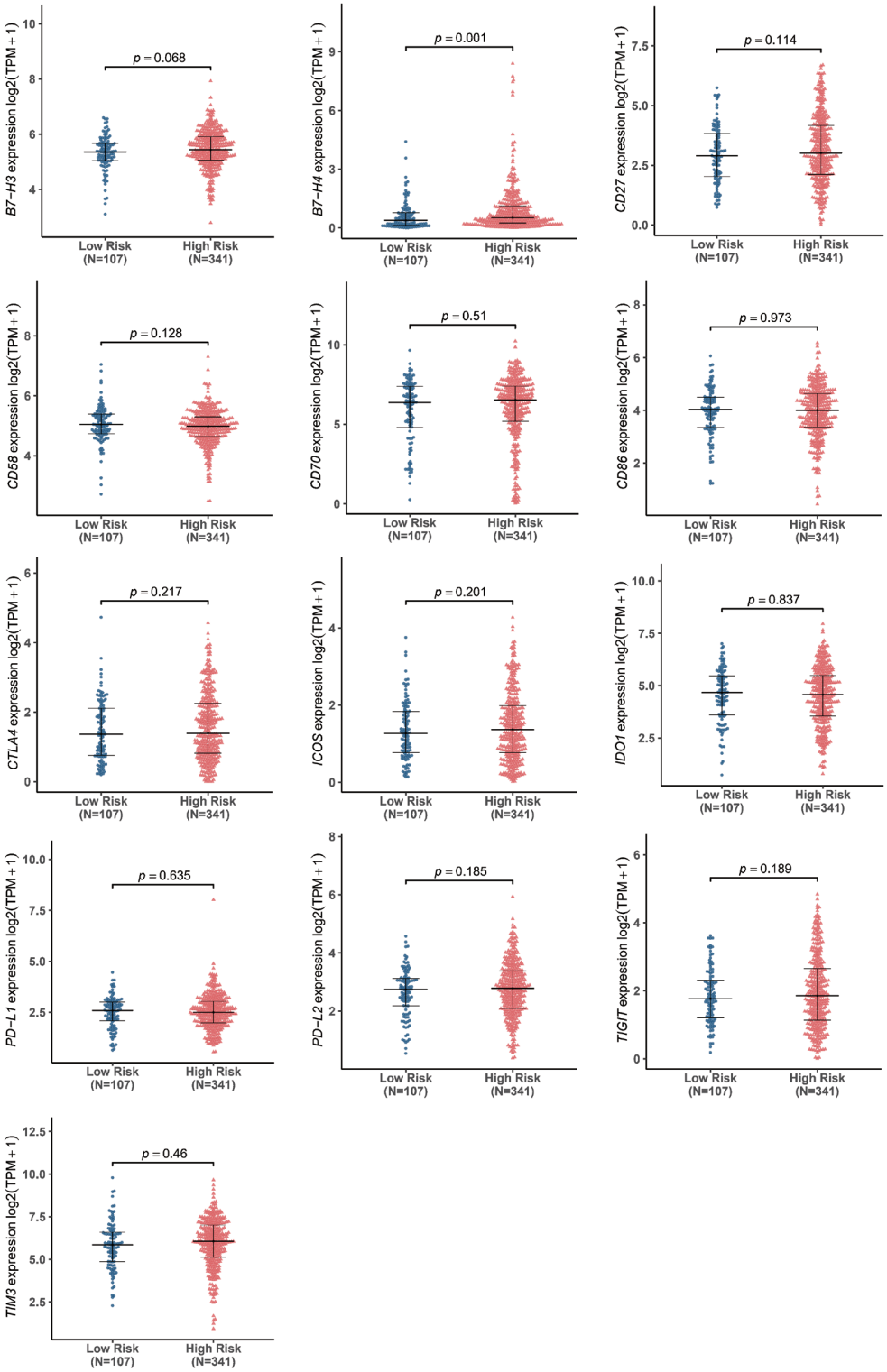

Figure S6 Expression levels of immune checkpoint molecules in patients in TCGA cohort identified with the 10-gene mutation classifier.

https://dx.doi.org/10.21037/tau-23-21